Supporting information

Conductive Nano Nickel Oxide/Hydroxide Paper Electrochemical Sensor for Serotonin Detection in Genetically Engineered *Drosophila*

Sharmila Prashanth [a], Manvitha Kadandelu [b], Shamprasad Varija.Raghu [b], K. Sudhakara Prasad,[a] Airody Vasudeva Adhikari [a,c]**

[a] Nano Material Research laboratory, Smart Materials and Devices, Yenepoya Research Centre, Yenepoya (Deemed to be University), Deralakatte, Mangalore 575 018, India

[b] Division of Neuroscience, Yenepoya Research Centre, Yenepoya (Deemed to be University), Deralakatte, Mangalore 575018, India

[c] Department of Chemistry, National Institute of Technology Karnataka, Surathkal, Mangalore 575025, India

Table of Contents

The RMS and mean roughness values increased from 10.04 ± 2.9 nm and 8.3 ± 2.6 nm (bare PPE) to 13.3 ± 5.2 nm and 10.4 ± 3.7 nm (Ppy-rGO), and significantly to 49.5 ± 18.1 nm and 38.5 ± 13.2 nm after NiO/Ni(OH)$_2$ deposition, respectively.The values are presented as mean ± standard deviation, calculated from multiple measurements across different surface regions using Gwyddion software. The substantial increase in roughness following each modification step suggests statistically relevant changes in surface morphology. These morphological features, including mountain-like ridges and increased thickness, contribute to an enhanced electroactive surface area, which is advantageous for electrochemical sensing. Detailed roughness parameters and thickness values, calculated using Gwyddion software, are provided in **Table S1**.

Modified electrode	RMS Roughness (nm)	Mean Roughness (nm)
Bare PPE	10.04 ± 2.9	8.3 ± 2.6
PPE-Ppy-rGO	13.3 ± 5.2	10.4 ± 3.7
PPE-Ppy-rGO-NiO/Ni(OH)$_2$	49.5 ± 18.1	38.5 ± 13.2

Table S1. AFM Data.

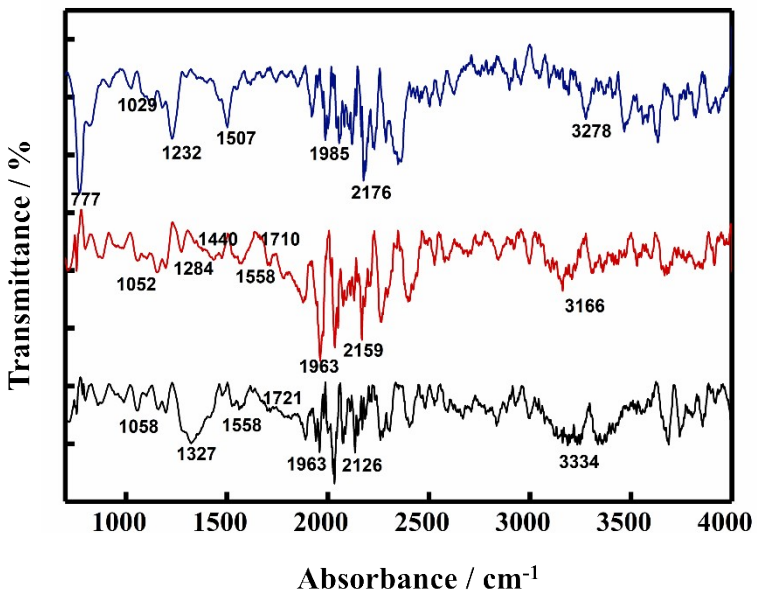

Figure S1. FT-IR spectra obtained for PPE **(black)**, PPE-Ppy-rGO **(red)**, and PPE-Ppy-rGO-NiO/Ni(OH)$_2$ **(blue)**

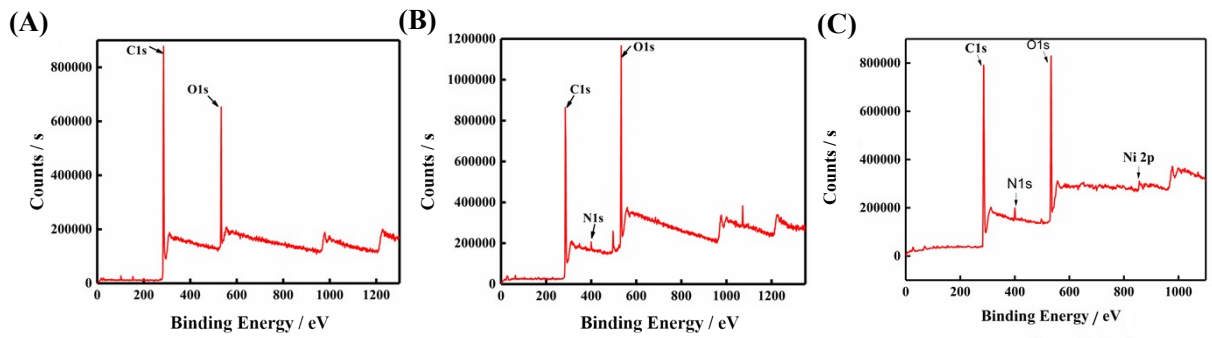

Figure S2. XPS Survey scan for (A) PPE (B) PPE-Ppy-Rgo (C) PPE-Ppy-rGO-NiO/Ni(OH)$_2$

Electrode	Atomic %				Atomic ratio		
	C1s	O1s	N1s	Ni2p	O1/C1	N1/C1	Ni/C1
PPE	82.99	17.01	-	-	0.0249	-	-
PPE-Ppy-rGO	71.71	26.91	1.38	-	0.375	0.0192	-
PPE-Ppy-rGO-NiO/Ni(OH)$_2$	73.61	23.62	1.99	0.79	0.227	0.026	0.011

Table S2. Atomic % and Atomic ratio calculated from the XPS data obtained for various electrodes.

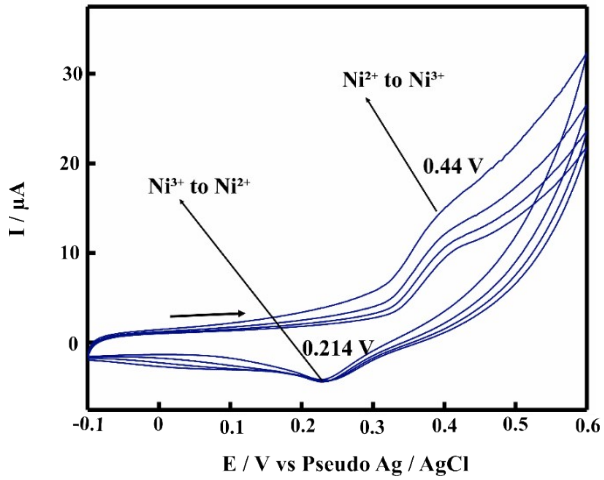

Figure S3. CV curves for the PPE-Ppy-rGO-NiO/Ni(OH)$_2$ nanocomposites electrodes, recorded over a potential range of –0.1 to 0.6 V at a scan rate of 0.05 V/s for 8 cycles in 0.1 M KOH

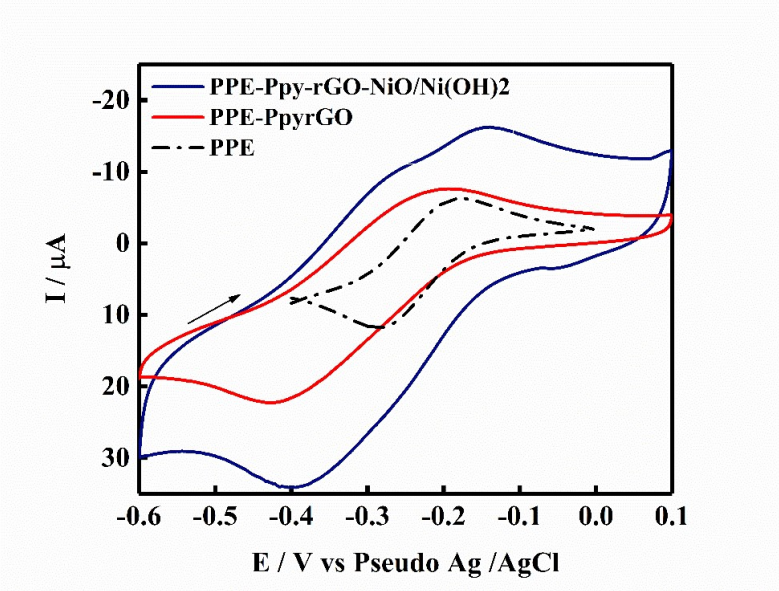

Figure S4. Cyclic voltammetry (CV) analysis of PPE, PPE-Ppy-rGO, and PPE-Ppy-rGO-NiO/Ni(OH)$_2$ in 1 mM $Ru(NH_3)_6Cl_3$ and 0.1 M KCl, measured at a scan rate of 0.05 V s^{-1}.

Electrochemical active surface area calculated using the Randles–Sevcik equation, where D calculated as from previous reports [1, 2]

Electrode	*Electroactive probe*	*D/cm²/s⁻¹*	*A_{geo}/cm²*	*A_{real}/cm²*	*% Real*
Bare PPE	$Ru(NH_3)_6Cl_3$	9.1 ×10 $^{-6}$	0.07	0.37	528.6
PPE-Ppy-rGO	$Ru(NH_3)_6Cl_3$	9.1 ×10 $^{-6}$	0.07	0.46	657.1
PPE-Ppy-rGO-NiO/Ni(OH)$_2$	$Ru(NH_3)_6Cl_3$	9.1 ×10 $^{-6}$	0.07	0.99	1414.3

Table S3. Electrochemical active surface area analysis of modified electrodes

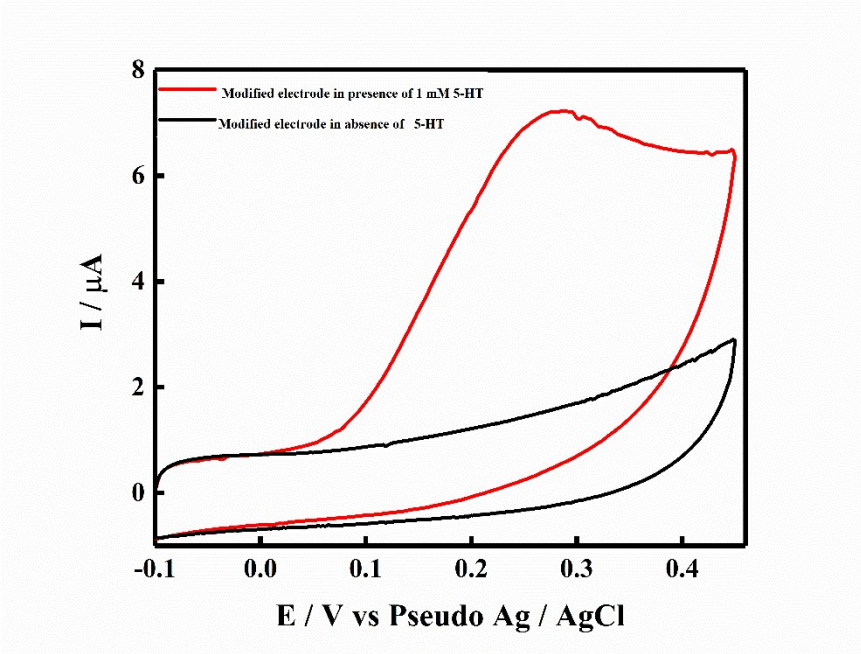

Figure S5. Cyclic voltammetry (CV) analysis of PPE-Ppy-rGO-NiO/$Ni(OH)_2$ in the absence (black) and in presence of 1 mM 5-HT 0.1 M PB solution (pH 7.4) (red) measured at a scan rate of 0.05 V s^{-1}.

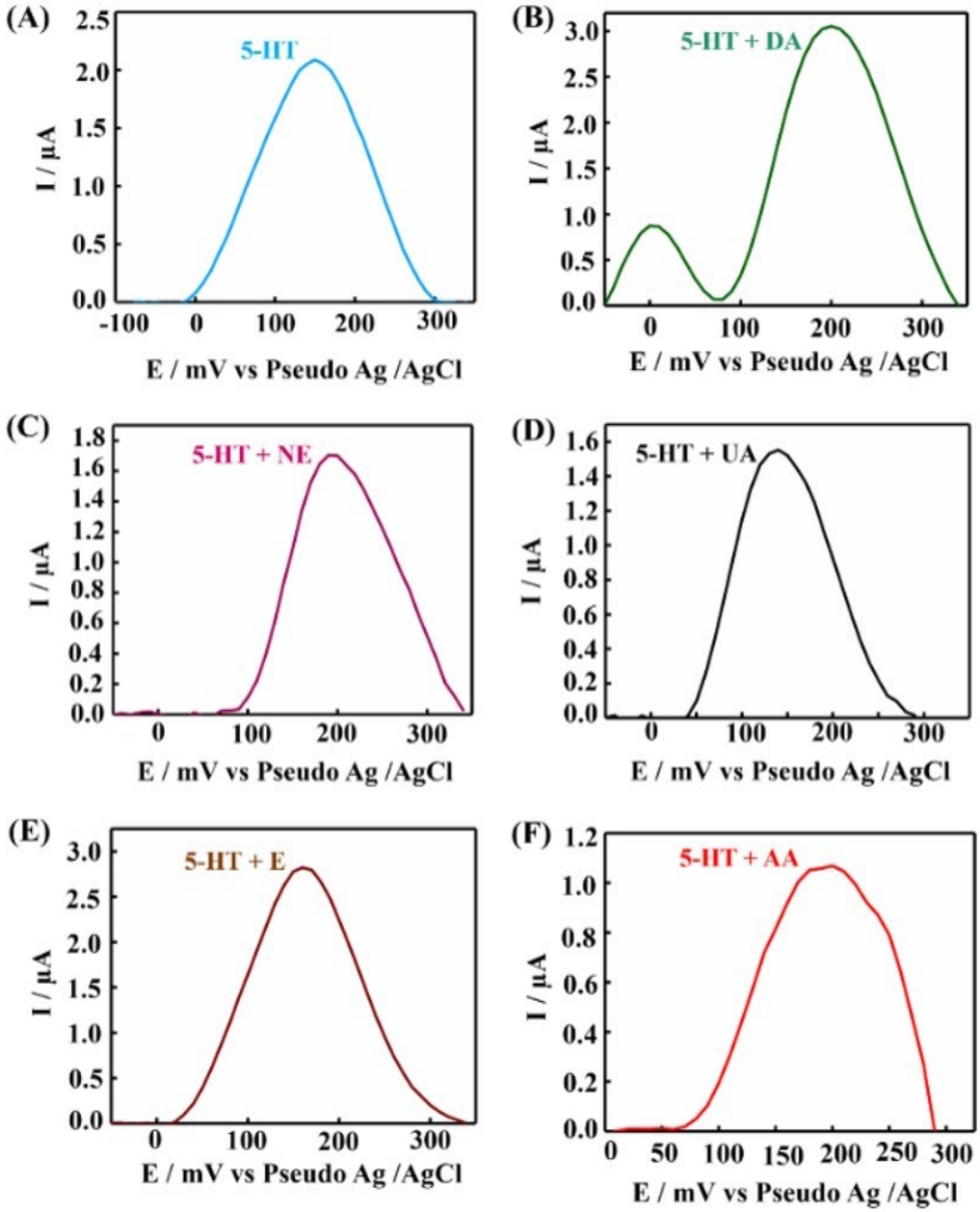

Figure S6. SWV for interference studies of the developed PPE-Ppy-rGO-NiO/Ni(OH)$_2$ sensor against various interfering species, (**A**) 5-HT (**B**) 5-HT + DA (**C**) 5-HT + NE (**D**) 5-HT + UA (**E**) 5-HT + E (**F**) 5-HT + AA each at a concentration of 100 µM with 5-HT.

Sensing materials	*Method of detection*	*Linear range*	*LOD nM*	*LOD ng/mL*	*Real samples analysed*	*Ref.*
Nb_2CT_x/PCN	DPV	1 µM – 100 µM	63.24	11.14	Human serum	3
Nafion-CNT/EC CFMEs	CV	100 µM – 800 µM	140	24.6	Artificial urine sample	4
FeC-AuNPs-MWCNT	SWV	0.05 µM – 20 µM	17	2.99	Urine sample	5
Aptamer-based biosensor	EIS	25 µM - 150 nM	5.6	0.99	-	6
Au-CNT membrane electrode	CV	0.5 µM – 10 µM	30	5.29	Cell media	7
Dy_2MoO_6 nanosheets	DPV	10 µM - 130 nM	340	59.9	Human blood and urine	8
RGO/p-PDA/β-$Ni(OH)_2$	Amperometry	5 µM - 325 µM	46.2	8.14	Urine	9
PPE-Ppy-rGO-Fe_2O_3	DPV	0.01 µM - 500 µM	22	*3.88*	*Drosophila melanogaster* brain sample	10
PPE-Ppy-rGO-Ni/$Ni(OH)_2$	SWV	0.007 nM - 0.48 nM 0.48 nM – 500 µM	0.024 383.7 nM	0.0042 67.61	Genetically modified *Drosophila melanogaster* brain sample	Present work

Table S4. Comparison of electrochemical performance of various reported electrodes.

Normal serotonin (5-HT) concentrations typically range from 270 to 1490 nM in serum, approximately 300 to 1650 nM in urine, and are markedly lower in cerebrospinal fluid (CSF), often below 0.0568 nM.[11-12]

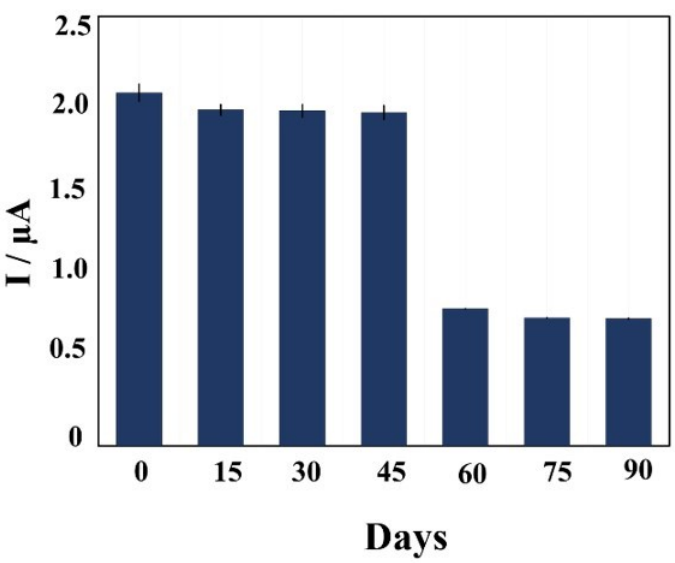

Figure S7. Histogram presenting the repeatability study for three PPE-Ppy-rGO- NiO/Ni(OH)$_2$ electrode.

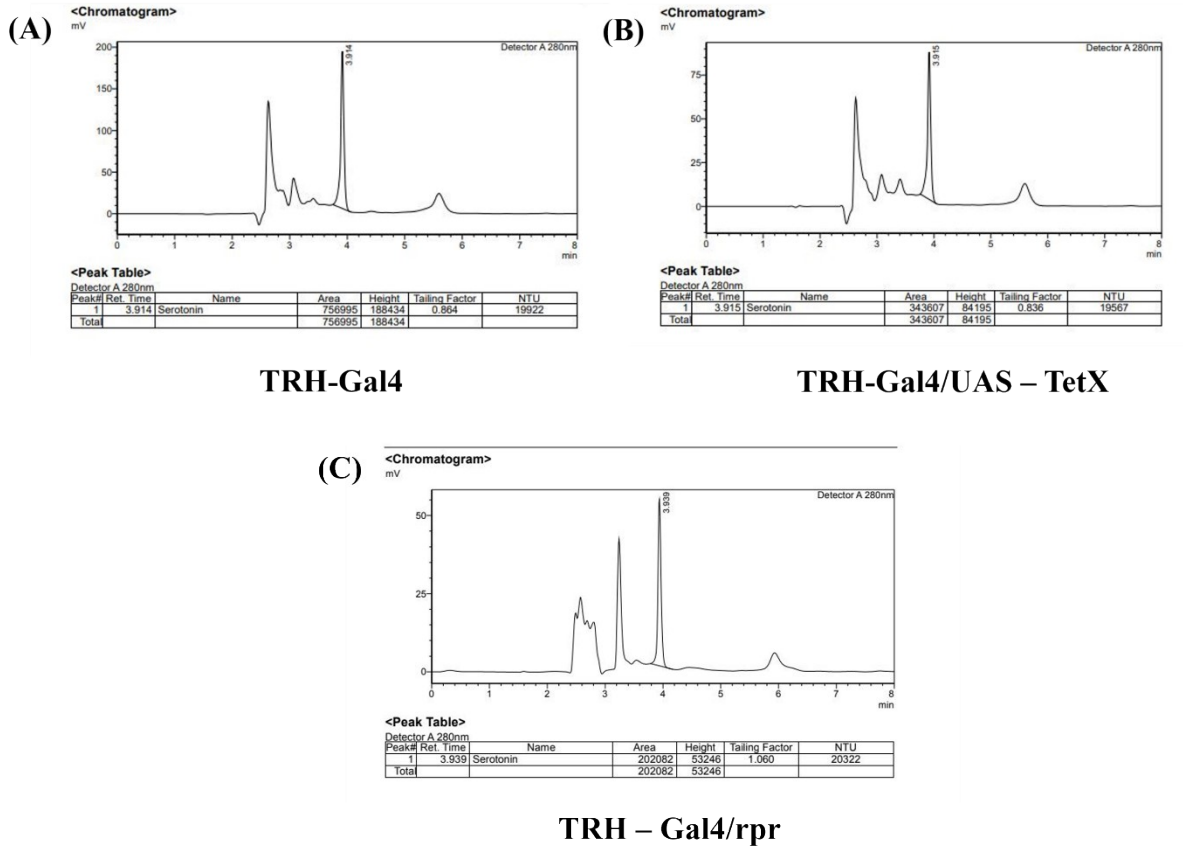

Figure S8. HPLC response for genetically engineered *Drosophila melanogaster* brain samples **(A)** TRH-Gal4 **(B)** TRH-Gal4/UAS-TeTxLC (**C)** TRH-Gal4/UAS-rpr

Sample (Genetically engineered *Drosophila melanogaster* brain sample)	Spikes	Added amount of 5-HT (µM)	Found amount Of 5-HT (µM)	Recovery (%)
TRH-Gal4	-	0.0	27.6	-
	1st spike	8	35	98.3
	2nd spike	7.0	42	98.6
	3rd spike	5.0	46.5	97.7
TRH-Gal4/UAS -TeTxLC	-	0.0	11.9	-
	1st spike	9.0	21	100.5
	2nd spike	7.0	27	96.8
	3rd spike	5.0	32.2	97.9
TRH-Gal4/UAS -rpr	-	0.0	7.59	-
	1st spike	8.3	15.6	98.1
	2nd spike	6.3	21.9	98.7
	3rd spike	5	27.3	100.4

Table S5. Spiked real sample analysis

References

(1) F. Marken, J. C. Eklund, R. G. Compton, *Journal of Electroanalytical Chemistry,* 1995, **395**, 335–39. https://doi.org/10.1016/0022-0728(95)04268-S.

(2) A. G.-M. Ferrari, C. W. Foster, P. J. Kelly, D. A. C. Brownson, and C. E. Banks, Biosensors 2018, 8, 53. https://doi.org/10.3390/bios8020053

(3) M. Mufeeda, M. Ankitha, and P. A. Rasheed, *ACS Applied Nano Materials,* 2023, ***6***, 21152–21161. https://doi.org/10.1021/acsanm.3c04222.

(4) J. Han, J. M. Stine, A. A. Chapin, and R. Ghodssi, *Analytical Methods* 2023, **15**, 1096–1104. https://doi.org/10.1039/D2AY01627C

(5) B. Wu, S. Yeasmin, Y. Liu, L.-J. Cheng, *Sensors and Actuators B: Chemical,* 2022, **354**, 131216. https://doi.org/10.1016/j.snb.2021.131216.

(6) H. M. N. Ahmad, A. Andrade, E. Song, *Biosensors* 2023, **13**, 983. https://doi.org/10.3390/bios13110983.

(7) A. A. Chapin, P. R. Rajasekaran, D. N. Quan, L. Hu, J. Herberholz, W. E. Bentley, R. Ghodssi, *Microsystems and Nanoengineering* **2020**, *6* (1), 1–13. https://doi.org/10.1038/s41378-020-00184-4.

(8) G. Singh, A. Kushwaha, M. Sharma, *Materials Chemistry and Physics* 2022, **279**, 125782. https://doi.org/10.1016/j.matchemphys.2022.125782.

(9) A. K. Mohiuddin, S. Jeon, *Sensors and Actuators A: Physical,* 2022, **348**, 113974. https://doi.org/10.1016/j.sna.2022.113974.

(10) S. Prashanth, R. A. Aziz, S. V. Raghu, Y.-B. Shim, K. S. Prasad, A. V. Adhikari, *Material Advances.* 2024, **5**, 1185-98. https://doi.org/10.1039/D3MA00777D

(11) M. Lindström, N. Tohmola, R. Renkonen, E. Hämäläinen, C. Schalin-Jäntti, O. Itkonen, *Clinica Chimica Acta*, 2018, **482,** 78–83, https://doi.org/10.1016/j.cca.2018.03.030

(12) K. Khoshnevisan, E. Honarvarfard, F. Torabi, H. Maleki, H. Baharifar, F. Faridbod, B. Larijani, M. R. Khorramizadeh, *Clinica Chimica Acta*, 2020, **501**,112-19. https://doi.org/10.1016/j.cca.2019.10.028.

243

244

245

246